The Astrophysical Journal, 802:16 (9pp), 2015 March 20 doi:10.1088/0004-637X/802/1/16

CAN VERY MASSIVE POPULATION III STARS PRODUCE A SUPER-COLLAPSAR?

Sung-Chul Yoon[1], Jisu Kang[1], and Alexandra Kozyreva[2]
[1] Department of Physics and Astronomy, Seoul National University, Gwanak-gu, Gwanak-ro1, 151-742, Seoul, Korea; yoon@astro.snu.ac.kr
[2] Argelander Institute for Astronomy, University of Bonn, Auf dem Hügel 71, D-53121, Bonn, Germany
Received 2014 September 13; accepted 2015 January 14; published 2015 March 16

ABSTRACT

A fraction of the first generation of stars in the early universe may be very massive ($\gtrsim$300 $M_\odot$) as they form in metal-free environments. Formation of black holes from these stars can be accompanied by supermassive collapsars to produce long gamma-ray bursts of a unique type having a very high total energy ($\sim 10^{54}$ erg) as recently suggested by several authors. We present new stellar evolution models of very massive Population III stars including the effect of rotation to provide theoretical constraints on super-collapsar progenitors. We find that the angular momentum condition for a super-collapsar can be fulfilled if magnetic torques are ignored, in which case Eddington–Sweet circulations play the dominant role for the transport of angular momentum. We further find that the initial mass range for super-collapsar progenitors would be limited to 300 $M_\odot \lesssim M \lesssim$ 700 $M_\odot$. However, all of our very massive star models of this mass range end their lives as red supergiants rather than blue supergiants, in good agreement with most of the previous studies. The predicted final fate of these stars is either a jet-powered type IIP supernova or an ultra-long, relatively faint gamma-ray transient, depending on the initial amount of angular momentum.

Key words: gamma-ray burst: general – stars: evolution – stars: Population III – stars: rotation – supernovae: general

1. INTRODUCTION

Population III stars are the main sources of ionizing photons and the only producers of heavy elements in the early universe. Their exact role on the reionization history and the chemical evolution largely depends on their initial mass functions. In the metal-free environment where the first stars form, thermal cooling of star-forming regions is dominated by hydrogen molecules, which are much less efficient coolants than heavy elements and dusts. It is therefore widely believed that Population III (Pop III) stars are systematically more massive than Pop II and Pop I stars (e.g., Abel et al. 2002; Bromm et al. 2002).

According to recent numerical simulations, most Pop III stars would have a mass range of 10–1000 $M_\odot$ (e.g., Omukai & Palla 2003; Bromm et al. 2009; Ohkubo et al. 2009; Hosokawa et al. 2011; Stacy et al. 2012; Hirano et al. 2014), while formation of more massive Pop III stars (>1000 $M_\odot$) still remains a good possibility (Hosokawa et al. 2012). A significant fraction of them would produce core-collapse supernovae for initial masses of 10–100 $M_\odot$, and pulsational pair-instability or pair-instability supernovae for 100–300 $M_\odot$ (Heger & Woosley 2002; Umeda & Nomoto 2002). According to the recent numerical simulations, the first stars may rotate at a velocity close to the critical rotation (Stacy et al. 2011, 2013), and these mass ranges can be significantly lowered if rapid rotation induces strong chemical mixing inside stars (Yoon et al. 2012; Chatzopoulos & Wheeler 2012; Glatzel et al. 1985). Gamma-ray bursts (GRBs) may also occur with sufficiently high initial angular momentum, for about 12–80 $M_\odot$ (Yoon et al. 2012). Detection of these events at $z \simeq 20$ with the next generation of telescopes will give us invaluable information on the nature of Pop III stars (e.g., Kawai et al. 2006; Greiner et al. 2009; Salvaterra et al. 2009; Tanvir et al. 2009; Cucchiara et al. 2011).

On the other hand, Pop III stars with initial masses of 300–50000 $M_\odot$ are supposed to directly collapse to a black hole (e.g., Fryer et al. 2001; Heger & Woosley 2002). In particular, those with $M_{\rm init} > 1000\,M_\odot$ are often considered seeds for super-massive black holes that are found at high redshift (e.g., Madau & Rees 2001; Schneider et al. 2002). Recently several authors suggested that formation of black holes in very massive stars can be accompanied by a super-collapsar (i.e., a collapsar with a black hole mass higher than a few hundreds of solar masses) to produce relativistic jets (Komissarov & Barkov 2010; Mészáros & Rees 2010; Suwa & Ioka 2011; Maio & Barkov 2014). Given that the considered black holes are very massive compared to the case of ordinary GRBs, there might be unique observational signatures from these super-collapars, depending on the details of the progenitor structure. For example, the amount of total energy released by jets could be significantly larger than those of ordinary GRBs (Komissarov & Barkov 2010; Mészáros & Rees 2010).

One of the key conditions for having a collapsar event is rapid rotation of the infalling matter onto the black hole, of which the specific angular momentum must be high enough to form an accretion disk (i.e., $j \gtrsim 10^{16} - 10^{19}\,{\rm cm^2\,s}$ for the black hole mass of 3–1000 $M_\odot$; Woosley 1993; MacFadyan & Woosley 1999): if the black hole mass is higher than a few hundreds of solar masses, the corresponding radius of the disk is too large for neutrino annihilation to produce a relativistic jet (MacFadyan & Woosley 1999). Therefore, another key ingredient for a super-collapsar is a strong magnetic field (i.e., $B \gtrsim 10^{13}$ G around the black hole) such that the rotational energy of the black hole may be extracted by the Blanford–Znajek mechanism (Komissarov & Barkov 2010; Mészáros & Rees 2010). The progenitors of super-collapsars should be both rapidly rotating and strongly magnetic.

Yoon et al. (2012, hearafter, YDL12) calculated evolutionary models of Pop III stars including rotation and magnetic fields. In their models the Tayler–Spruit (TS) dynamo (Spruit 2002) plays a key role in transporting angular momentum inside stars. Because of the efficient angular

momentum transport from the convective core to the outer layers via magnetic torques, stars can maintain near-rigid rotation throughout the main sequence and lose angular momentum via mass shedding as the surface reaches critical rotation. This effect becomes more important for a very massive Pop III star of which the surface luminosity is close to the Eddington limit because it can reach the critical rotation even with a fairly low rotation velocity. As a result, Pop III stars more massive than about 300 $M_{\odot}$ cannot retain enough angular momentum to produce a super-collapsar according to YDL12.

The TS dynamo adopted by YDL12 is one of the most considered explanations for the rapid transport of angular momentum in radiative layers of stars, which is implied by a number of observations, in particular with low-mass stars (e.g., Eggenberger et al. 2005, 2012; Suijs et al. 2008; Cantiello et al. 2014). However, the efficiency of the TS dynamo is still a matter of debate in the community (Braithwaite 2006; Zahn et al. 2007; Denissenkov et al. 2010; Arlt & Rudiger 2011). The strong braking implied in low-mass stars might be instead related to some other mechanisms like internal gravity waves (Zahn et al. 1997; Talon et al. 2002), which have not been well understood in the context of massive stars and thus might not be necessarily relevant. If the transport of angular momentum in massive stars is much less efficient than what is predicted with the TS dynamo, they could retain a large amount of angular momentum inside the core, while magnetic fields of large scales might be generated in convective layers before collapse or in the accretion disk after black hole formation, thus fulfilling the necessary conditions for a super-collapsar. Given the importance of super-collapsar events as a probe on the nature of Pop III stars, it is worthwhile to investigate this possibility in some detail to provide a theoretical boundary condition for super-collapsar progenitors. For this purpose, we present new evolutionary models of very massive Pop III stars ($M_{\rm init} \gtrsim 300\,M_{\odot}$) without magnetic torques according to the TS dynamo. This means that we only consider Eddington–Sweet circulations and other hydrodynamic instabilities for the transport of angular momentum.

We briefly explain the numerical methods used for our models in Section 2. In the section that follows (Section 3), we describe the properties of very massive Pop III stars on the zero-age main sequence (ZAMS). In particular, we show that the angular momentum condition for a collapsar becomes more difficult to meet for a higher initial mass because the Eddington factor at the stellar surface becomes larger. In Section 4, we present the evolutionary models including rotation and discuss the initial conditions of Pop III stars needed for super-collapsar progenitors. We discuss the implications of our results for the final fate of super-collapsar progenitors and the relevant uncertainties of our models in Section 5. We conclude our discussions in Section 6.

2. NUMERICAL METHODS

We used the one-dimensional hydrodynamic stellar evolution code that is described in YDL12 and Kozyreva et al. (2014). This code implicitly solves the stellar structure equations for which the Henyey-type method is adopted. The OPAL opacity table (Iglesias & Rogers 1996) is used for $T > 10^4$ K and the prescription by Alexander & Ferguson (1994) for lower temperatures. We follow Endal & Sofia (1976) to consider the effect of the centrifugal force on the stellar scructure and Heger et al. (2000, 2005) for the redistribution of angular momentum, which is approximated as a diffusive process. We used the same physical parameters for convection, semi-convection, and rotationally induced chemical mixing and transport of angular momentum, but the TS dynamo is not included in the present study except in one model sequence. This means that the considered transport processes due to rotation include Eddington–Sweet circulations; the secular shear instability; and the Goldreich, Schubert, and Fricke (GSF) instability as explained in Heger et al. (2000). The overshooting is applied for 0.335 times local pressure scale heights above the convectively unstable core and the adopted semi-convection parameter ($\alpha_{\rm semi}$; Langer et al. 1983) is 1.0, following Brott et al. (2011). Compared to YDL12, the nuclear network was improved to treat silicon burning as discussed in Kozyreva et al. (2014) and Kozyreva (2014). In some of our models, the silicon burning was followed with 13 main isotopes. In this way the main alpha-chain can be described without considering neutronization which does not play an important role in the structure of very massive stars undergoing pair-instability.

The treatment of mass loss for Pop III stars and its physical justification are fully described in YDL12. In short, the mass loss in our models is dominated by centrifugally driven mass shedding, which is treated as the following:

$$\dot{M}(v) = \max\left[10^{-14}\,M_{\odot}\ {\rm yr}^{-1}, \dot{M}(v=0)\right]\left(\frac{1}{1-\Omega}\right)^{0.43}, \quad (1)$$

where

$$\Omega := \frac{v}{v_{\rm crit}} \ \text{and} \ v_{\rm crit} = \sqrt{\frac{GM}{R}(1-\Gamma)}. \quad (2)$$

The critical rotation $v_{\rm crit}$ represents the modified Keplerian limit considering the effect of radiation when the stars approach the Eddington limit, for which the Eddington factor Γ is given by $\kappa L/(4\pi GMc)$. $\dot{M}(v=0)$ is the wind mass loss rate for the non-rotating case, for which we followed Kudritzki et al. (1989) and Nieuwenhuijzen & de Jager (1990) for $T_{\rm eff} > 10^4$ and $T_{\rm eff} \leqslant 10^4$, respectively, with a metallicity dependence of $Z^{0.69}$. Here, the metallicity means the total mass fraction of CNO elements at the surface and in this way the enhancement of the mass loss rate resulting from surface enrichment of heavy elements by chemical mixing is taken into account (see YDL12 for more discussion on this issue).

3. PROPERTIES ON THE ZAMS

Before presenting the evolutionary models, here we discuss the properties of very massive Pop III stars on the ZAMS. In Table 1, we provide the information on the ZAMS models for the mass range of 300–20,000 $M_{\odot}$. Here we assume that stars on the ZAMS rotate as a solid body, which can be justified because of the expected rapid transport of angular momentum in chemically homogeneous stars by convection and Eddington–Sweet circulations (e.g., Haemmerlé et al. 2013, see also the discussion below).

The surface luminosities of these very massive stars are close to the Eddington limit: the Eddington factor varies from $\Gamma = 0.774$ at $300\,M_{\odot}$ to $\Gamma = 0.996$ at $20{,}000\,M_{\odot}$. In consequence, these stars cannot have a very high critical rotation velocity, and the total amounts of angular momentum should be limited accordingly. The corresponding $v_{\rm crit}/v_{\rm K}$

Table 1
Physical Properties of the ZAMS Models

M_i	T_{eff}	$\log L/L_\odot$	Γ	v_{crit}/v_K	$\log J$	j	k
($M_\odot$)	(10^3 K)				(erg s)	(10^{19} cm^2 s^{-1})	
300	106.6	6.8	0.774	0.48	54.74	0.93	0.134
500	108.9	7.1	0.836	0.40	55.05	1.13	0.130
1000	110.7	7.5	0.885	0.32	55.46	1.46	0.122
2000	111.3	7.8	0.927	0.25	55.86	1.83	0.114
3000	111.3	8.0	0.954	0.22	56.08	2.04	0.110
4000	111.2	8.1	0.964	0.19	56.24	2.19	0.107
5000	111.1	8.2	0.970	0.17	56.36	2.31	0.104
7000	110.7	8.4	0.978	0.15	56.54	2.47	0.100
10,000	110.3	8.5	0.986	0.12	56.70	2.50	0.096
20,000	108.4	8.9	0.996	0.06	56.88	1.92	0.085

Note. Each column has the following meaning: M_i: initial mass, T_{eff}: effective temperature in units of 10^3 K, $\log L/L_\odot$: surface luminosity in units of the solar luminosity, Γ: Eddington factor at the surface, v_{crit}/v_K: the critical rotation for the given Γ at the equatorial surface in units of the Keplerian value with rigid rotation, $\log J$: the total angular momentum at the critical rotation, j: the specific angular momentum at the critical rotation, k: the dimensionless radius of gyration at the critical rotation (i.e., $J = kv_{crit}MR$).

($=\sqrt{1-\Gamma}$; see Equation (2)) with solid-body rotation changes from 0.48 to 0.06. Because the stellar radius is larger with higher mass, both the total angular momentum and the specific angular momentum at the critical rotation gradually increase with increasing mass up to about 10,000 $M_\odot$, despite the fact that v_{crit}/v_K decreases. However, v_{crit}/v_K becomes so small for 20,000 $M_\odot$ that the specific angular momentum becomes smaller than that of a 10,000 $M_\odot$ star. Another factor that limits the amount of angular momentum is the change of stellar structure as Γ approaches zero. The dimensionless radius of gyration (i.e., $k = J/(v_{rot}MR)$; see Table 1) decreases with increasing mass and therefore the amount of angular momentum for a given set of v_{crit}, M, and R should decrease as well.

This property leads to the following important conclusion: Pop III stars with $M_i > 3000\ M_\odot$ at their birth cannot contain enough angular momentum in their cores to produce a collapsar because of the effect of high radiation pressure, as illustrated in Figure 1. Only the outermost layers have specific angular momentum above the critical limit in these stars, and therefore production of an energetic GRB cannot occur (see discussion below). This fact is based only on the structure of Pop III stars on the ZAMS and does not depend on the uncertain physical processes like mass loss that has strong impact on the stellar evolution. This gives a strong upper mass limit for super-collapsar progenitors. Given that $M_i \gtrsim 300\ M_\odot$ is required to avoid a pair-instability explosion, only Pop III stars in the mass range of $300\ M_\odot \lesssim M_i \lesssim 3000\ M_\odot$ can be considered potential super-collapsar progenitors that can produce an energetic GRB, in terms of the initial angular momentum budget. Therefore, this result effectively rules out the possibility of an energetic gamma-ray burst with formation of intermediate-mass black holes of $\sim 10^4\ M_\odot$ from super-massive Pop III stars that can be seeds for super-massive black holes in high-redshift quasars (cf. Spolyar et al. 2009; Freese et al. 2010).

4. EVOLUTIONARY MODELS

We calculated evolutionary models for 300, 500, 700, 1000, and 2000 $M_\odot$ including rotation but without the TS dynamo as summarized in Table 2. We exceptively included the TS dynamo in the sequence S300M that shares the same initial condition with S300C, for comparison. It is well known that these very massive stars undergo the pair instability when the central temperature exceeds about 10^9 K, which leads to rapid contraction of the core and consequent rapid oxygen and silicon burning on a dynamical timescale. Because of the very high binding energy, this explosive nuclear burning cannot make these stars explode to produce a supernova. This pair instability phase was followed until $T_c = 5.4 \times 10^9$ K and $T_c = 6.9 \times 10^9$ K for S300C and S500C respectively, which are good candidates for super-collapsar progenitors. Although these end points still did not reach the pre-collapse stage ($T_c \sim 10^{10}$K), we did not continue the calculation because of a numerical difficulty mainly caused by very small timesteps encountered at such high temperature at the center. For the other model sequences, the calculation was terminated immediately before/at the onset of the pair instability ($T_c = 5 \times 10^8 \cdots 10^9$ K), beyond which the evolutionary time is too short to have any further significant redistribution of angular momentum. We find that the chemically homogeneous evolution (CHE) does not occur in any of our model sequences (see YDL12 for a detailed discussion on the condition of the CHE).

As shown in Figure 3, most of the ZAMS models of the considered mass range have a sufficient amount of angular momentum to produce a collapsar, such that any layer of them could form an accretion disk around the black hole that would be made below it. As mentioned above, these stars on the ZAMS rotate as a solid body. As hydrogen burning in the core develops, differential rotation across the boundary between the contracting convective core and the expanding radiative envelope would be created without any transport of angular momentum. However, they undergo rapid redistribution of angular momentum mostly via convection and Eddington–Sweet circulations as long as the chemical stratification inside stars is not significant. Convection leads to rigid rotation in the convective core on the dynamical timescale, and Eddington–Sweet circulations in chemically homogeneous layers occur on the thermal timescale which is much shorter than the evolutionary timescale[3].

For example, in the sequence S300C, solid-body rotation is maintained fairly well until the central helium mass fraction

[3] We find that the role of the secular shear instability and the GSF instability is minor in our models.

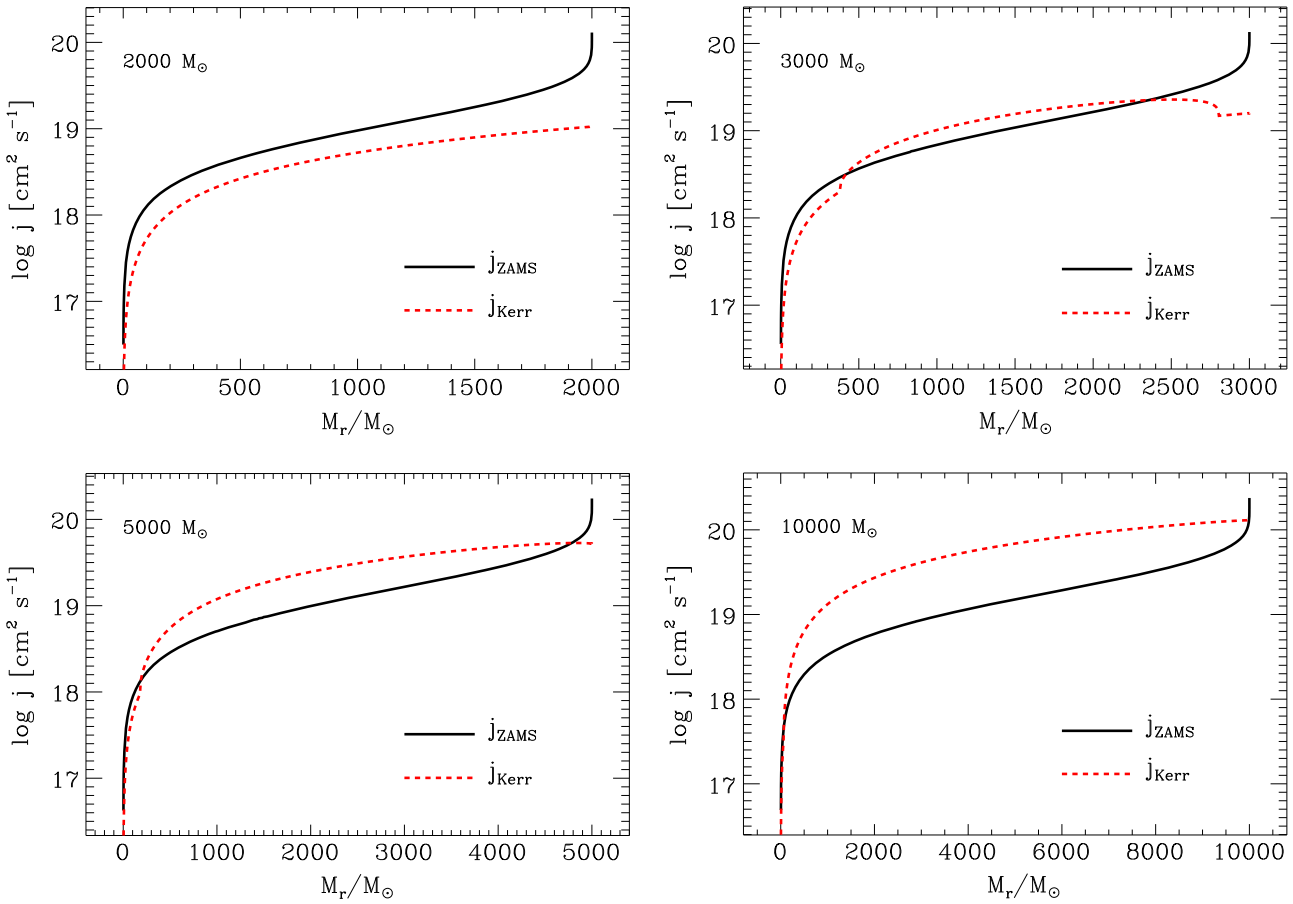

Figure 1. Specific angular momentum distribution in the Pop III models on the ZAMS for 2000, 3000, 5000, and 10,000 $M_{\odot}$, as a function of the mass–coordinate (solid line), compared to the specific angular momentum at the last stable orbit around the Kerr black hole that would form with the given mass and angular momentum (dashed line).

Table 2
Physical Properties of the Evolutionary Models

Sequation No.	M_i	v_i	v_i/v_c	log J_i	$T_{c,f}$	M_f	$T_{eff,f}$	R_f	log J_f	M_{He}	a_{He}
	($M_{\odot}$)	(km s^{-1})		(erg s)	(10^9 K)	($M_{\odot}$)	(K)	($R_{\odot}$)	(erg s	($M_{\odot}$)	
S300A	300.0	274.0	0.2	53.9	1.0	298.5	4380	5563.7	53.7	153.8	0.6
S300B	300.0	536.8	0.4	54.2	1.0	291.5	4081	5179.2	53.8	158.3	0.9
S300C	300.0	1276.2	0.9	54.6	5.4	264.0	4271	4769.8	53.8	200.9	1.0
S300M	300.0	1276.2	0.9	54.6	0.6	258.1	4442	5642.9	53.2	189.7	0.1
S500A	500.0	454.5	0.4	54.4	0.9	493.0	4458	7530.7	54.3	254.4	0.6
S500B	500.0	598.6	0.5	54.6	0.9	492.1	4348	7912.7	54.3	258.6	0.9
S500C	500.0	1110.8	0.8	54.9	6.9	464.9	4157	7022.7	54.4	276.8	1.0
S700A	700.0	1110.6	0.8	55.1	0.9	627.9	4508	8650.9	54.6	417.8	0.9
S700B	700.0	1384.1	1.0	55.2	0.9	615.8	4135	8246.1	54.6	376.9	0.9
S1000A	1000.0	1166.2	0.9	55.3	1.1	868.0	3908	11041.9	54.4	492.2	0.6
S2000A	2000.0	1115.5	1.0	55.7	0.5	1758.2	5353	10291.0	54.7	1250.0	0.3

Note. Each column has the following meaning: M_i: initial mass, v_i: initial rotational velocity at the equatorial surface, v_i/v_c: ratio of the initial rotational velocity to the critical velocity, log J_i: initial total angular momentum, $T_{c,f}$: central temperature at the end of calculation, M_f: final mass, $T_{eff,f}$: final effective temperature, R_f: final radius, log J_f: final total angular momentum, M_{He}: mass of the helium core (i.e., the total mass below the hydrogen envelope) at the end of the calculation, a_{He}: Kerr parameter of the black hole that the entire helium core would make as a result of collapse.

reaches about 0.75 (the top-left panel of Figure 2). The star reaches the critical rotation soon after the onset of core hydrogen burning because of this rapid transfer of angular momentum and the gradual increase in the radius and surface luminosity, and therefore loses angular momentum by the resulting mass loss. However, the angular momentum transfer from the core to the envelope via Eddington–Sweet circulations is significantly slowed down when the chemical stratification becomes strong across the boundary between the core and the envelope (the so-called μ—barrier; Meynet & Maeder 1997). Angular momentum can be effectively trapped in the core in this way and the degree of differential rotation between the core and the envelope becomes gradually stronger (Figure 2). The final model of S300C

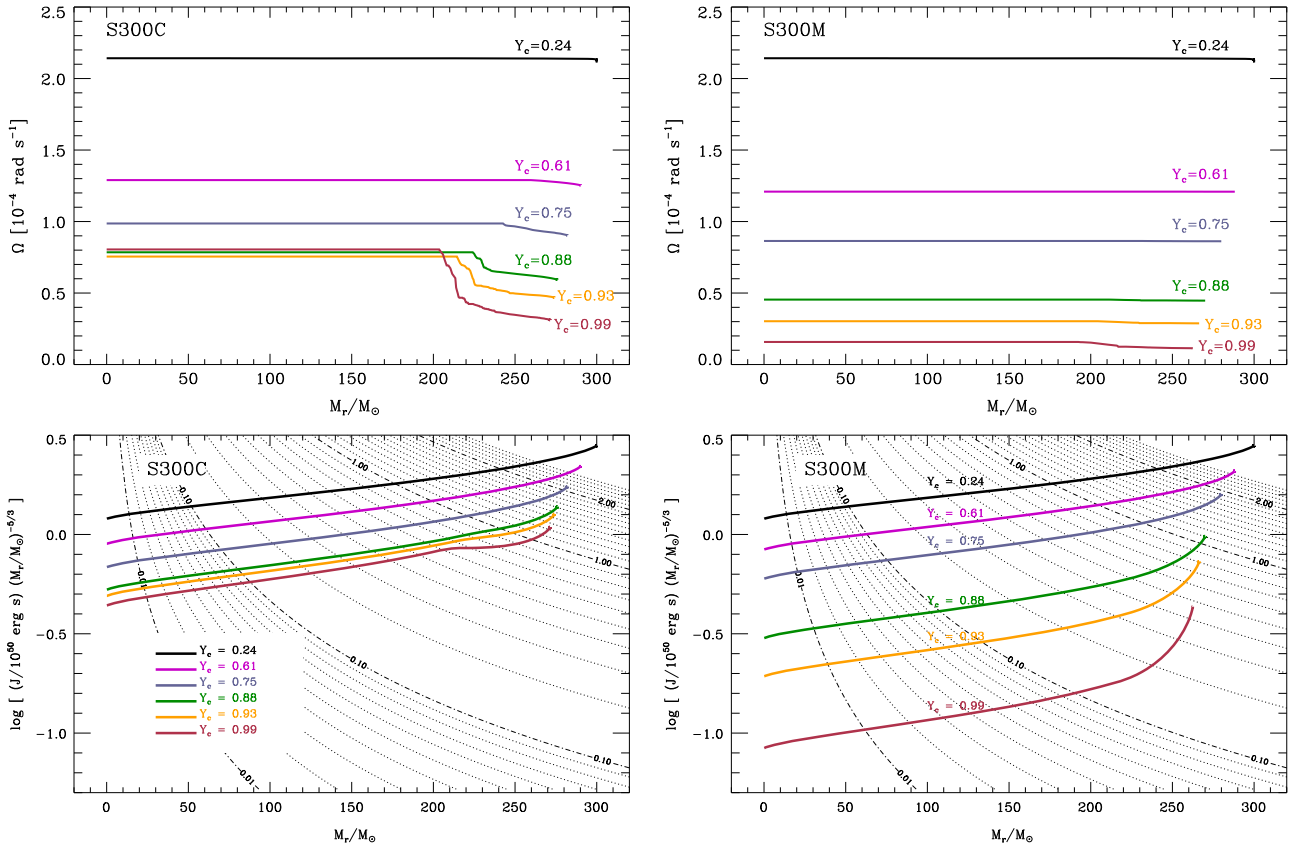

Figure 2. Top panels: evolution of angular velocity on the main sequence in S300C (left panel) and S300M (right panel), respectively. The label Y_c marks the central mass fraction at the given evolutionary time of each profile. Bottom panels: the corresponding integrated angular momentum ($J(M_r) = \int_0^{M_r} j(m)dm$) profiles divided by $M_r^{5/3}$. (The evolution of the angular momentum inside stars is better visualized with $J(M_r)/M_r^{5/3}$ than with $J(M_r)$ as discussed by Heger et al. (2000).) The thin contour lines denote levels of constant angular momentum in units of 10^{50} erg s.

retains enough angular momentum to produce a collapsar (Figure 3).

In the corresponding magnetic model sequence S300M, magnetic torques via the TS dynamo are strong enough to overcome the μ—barrier and near-rigid rotation is maintained until the end of the main sequence (top-right panel of Figure 2). As a natural consequence, this star loses more angular momentum than in S300C (bottom panels in Figure 2). In contrary to the corresponding non-magnetic model, the final model of S300M does not retain enough angular momentum for a collapsar to occur (see YDL12 for more comprehensive discussion on magnetic Pop III star models).

The initial mass is another key factor for determining the final outcome. The envelopes of more massive stars expand more rapidly both on the main sequence and during the post-main sequence phases (Marigo et al. 2003; Yoon et al. 2012) and the amount of angular momentum carried away by mass loss, which is proportional to R^2, becomes larger. In consequence, Figure 3 indicates that the conditions for collapsar at the final stage can be fulfilled only for $M_i \lesssim 700\ M_\odot$. From this result, we conclude that the initial mass range for potential super-collapsar progenitors is $300\ M_\odot \lesssim M_i \lesssim 700\ M_\odot$.

5. IMPLICATIONS FOR SUPERNOVAE AND GAMMA-RAY BURSTS FROM SUPER-COLLAPSARS

All of our very massive Pop III star models become a red supergiant (RSG; Table 2). It is well known that a jet produced in the stellar core via a collapsar cannot easily penetrate an RSG envelope and therefore our models may not be good progenitors of GRBs, unfortunately. To investigate the possibility of a GRB from our super-collapsar progenitors in more detail, we made an estimate on the accretion rate from the disk that the rapidly rotating layers would make around the black hole, for the last models of S500A and S500C as shown in Figure 4. Here we followed the approximation by Woosley & Heger (2012):

$$\dot{M} = \frac{2M_r}{\tau_{\rm ff}}\left(\frac{\rho}{\bar{\rho} - \rho}\right), \quad (3)$$

where $\bar{\rho} = 3M_r/(4\pi r^3)$ and $\tau_{\rm ff} = 1/\sqrt{24\pi G\bar{\rho}}$. Although the last model of S500C is fairly close to the pre-collapse stage, the density of the core would further increase until the formation of the black hole, and the accretion rate from the core material given in the figure should be considered a lower limit. The sequence S500A was terminated at the onset of carbon burning (see Table 2), which is still far from the pre-collapse stage, but the core does not retain enough angular momentum for collapsar in this case. The accretion rate from the envelope in both S500A and S500C should not be affected by this uncertainty, because the hydrogen envelope has a much larger dynamical timescale than that of the core as shown in the figure.

The figure indicates that there would be three phases of mass accretion via an accretion disk in S500C. The first two would

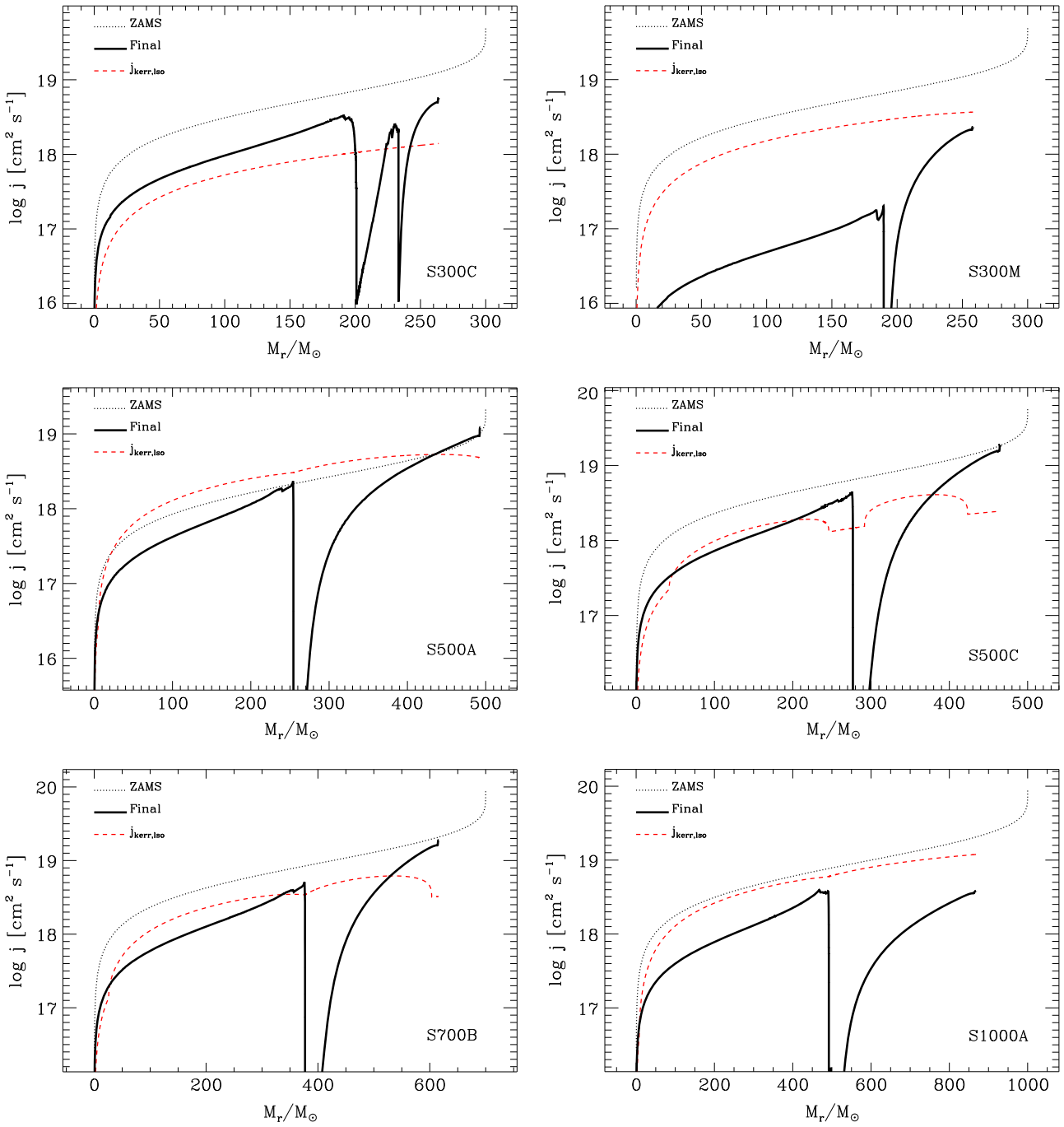

Figure 3. Mean specific angular momentum over the shells. The initial and final distributions of specific angular momentum are given by the dotted and solid lines, respectively. The dashed line denotes the specific angular momentum for the last stable orbit around a Kerr black hole having all mass and angular momentum below the given mass coordinate.

be made by accretion from the infalling matters of $3\,M_\odot \lesssim M_r \leqslant 47\,M_\odot$ (assuming the minimum black hole mass of $3\,M_\odot$) and of $204\,M_\odot \leqslant M_r \leqslant 277\,M_\odot$, and the last one from that of the hydrogen envelope ($379\,M_\odot \leqslant M_r \leqslant 465\,M_\odot$). The expected accretion rate in the core is very high, implying a production of a very powerful jet. However, the lifetime of the engine powered by the core material would be very short. Most of the core material below $M_r = 277\,M_\odot$ would be accreted onto the black hole within a second. The outermost layer of the core around $M_r = 270 - 277\ M_\odot$ has a relatively low accretion rate, but the accretion time may not exceed 100 s. This is much shorter than the jet crossing time through the hydrogen envelope ($\tau_{\rm cross} \sim R_*/c \sim 10^4$ s), posing a serious obstacle for the jet penetration and a GRB is not expected from the jet produced by the core.

The most interesting question may be whether or not a GRB-like event can be made by the disk accretion of the matter in the layers of $434\,M_\odot \leqslant M_r \leqslant 493\,M_\odot$ and $379\,M_\odot \leqslant M_r \leqslant 465\,M_\odot$ of the hydrogen envelopes in S500A and S500C, respectively. In particular, the expected accretion rate rapidly increases near the surface in Figure 4, which results from the density inversion in this layer (see Woosley & Heger 2012 for more discussion

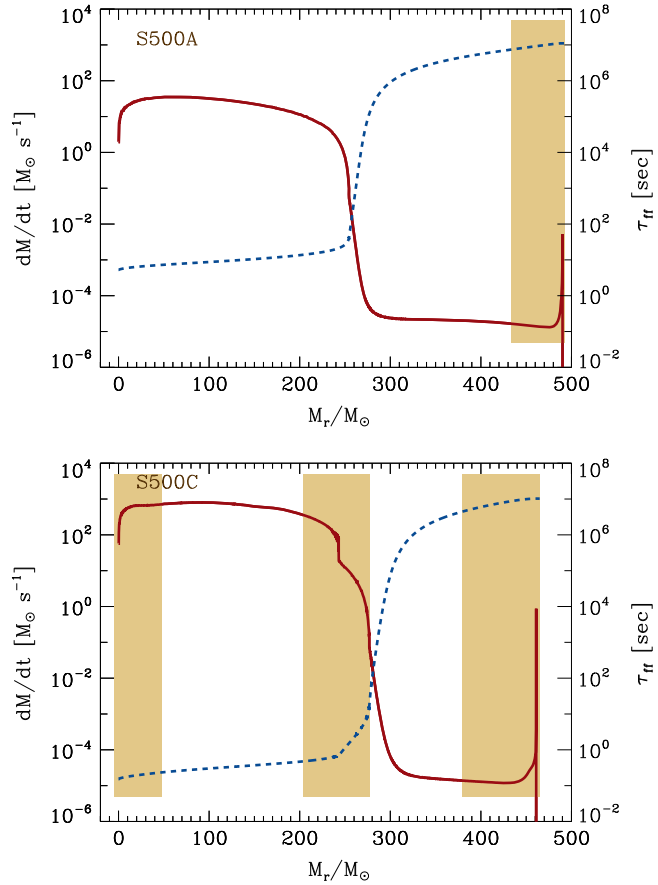

Figure 4. Expected mass accretion rate onto the black hole (solid line) given by Equation (3) as a function of the mass coordinate in the last models of S500A (upper panel) and S500C (bottom panel). The dashed line denotes the corresponding free-fall timescale ($\tau_{\rm ff} = 1/\sqrt{24\pi G\bar{\rho}}$, see the text). The rapidly rotating layers for which the specific angular momentum is higher than the critical value for the formation of a Keplerian disk (see Figure 3) are marked by the color shading.

on the effect of the density inversion). For the case of S500C, a GRB-like event is not likely to occur. The energy of the jets from the core injected into the hydrogen envelope would be higher than 10^{53} erg, if we assume the accretion-to-jet conversion efficiency of about $\eta = 10^{-3}$ following Suwa & Ioka (2011). Given that $\tau_{\rm cross} \ll \tau_{\rm ff}$, the forward shock of the jet from the core would become spherical by the time of its breakout from the envelope. Because the binding energy of the hydrogen envelope is only about 10^{51} erg, the whole hydrogen envelope would be blown away by the shock heating, preventing accretion of the outer envelope matter onto the black hole. The final outcome would be a jet-driven supernova of Type IIP rather than a GRB.

By contrast, for the case of S500A, the inner layers are not rapidly rotating, and expected to directly collapse to a black hole without making a jet. The outermost layers of the hydrogen envelope around the equatorial plane could be accreted onto the black hole via an accretion disk to produce a GRB-like event about two weeks after the collapse. In this case, with $\eta = 10^{-3}$, the gamma-ray transient would have $L \sim 10^{47}$ erg s^{-1} lasting for about a month. During the last few seconds, the accretion rate would dramatically increase as shown in Figure 4, resulting in $L \sim 10^{49}$ erg s^{-1}.

The above discussion is based on the S500A and S500C model, but the overall conclusion would be the same with the other progenitor models: a GRB is generally very difficult to produce from very massive Pop III stars because of the red supergiant envelope. Collapsar events in the inner layers would produce a jet-powered type IIP supernova if the initial rotation velocity of the progenitor were close to the critical limit. In a relatively slowly rotating progenitor, the core would not retain enough angular momentum for a collapsar, but a gamma-ray transient could be produced with the rapidly rotating outermost layers of the hydrogen envelope. This event would be marked by a long-lasting phase with a relatively low luminosity ($L \sim 10^{47}$ erg s^{-1} depending on η), which may resemble Swift 1644 + 57 (Burrows et al. 2011; Levan et al. 2011; Quataert & Kasen 2012), followed by a short phase of a few seconds having an enhanced luminosity by factors of 10^2–10^4 depending on the detailed structure of the layer with density inversion, in the rest frame. Such a transient from redshift of $z \sim 20$ would be bright in X-ray bands and last for a few years in the observer's frame. Given that $L \gtrsim 10^{52}$ erg s^{-1} is needed for a GRB from redshift of about 20 to be detected by the X-ray detector BAT (Komissarov & Barkov 2010), the predicted gamma-ray luminosity is too low to be observed in the near future, unfortunately.

One uncertain factor in our models is the mass-loss rate from very massive Pop III stars during the red supergiant phase. If the whole hydrogen envelope were stripped off before the collapse, favorable conditions for GRB production would be more easily fulfilled for the progenitors with rapidly rotating cores. As explained above, we considered enhancement of mass loss due to surface enrichment of heavy elements via chemical mixing by extrapolating the mass-loss rate given by Nieuwenhuijzen & de Jager (1990). In all of our models, the surface metallicity remains smaller than about a few times 10^{-7}, and the consequent enhancement of the mass loss rate is not significant. The mass loss rate might be further influenced by pulsational instabilities that can easily occur in stars close to the Eddington limit. Baraffe et al. (2001) concluded that mass loss induced by pulsation would not be efficient: only about 24 $M_\odot$ is expected to be lost from a 500 $M_\odot$ star. This is not significant compared to the amount of the lost mass in our models. However, the mechanism of RSG winds and its dependence on the surface abundance of CNO elements are not well understood yet and remains the biggest uncertain factor in our conclusions.

Another issue that is worth discussion is the final structure of very massive stars. Suwa & Ioka (2011) and Nagakura et al. (2012) showed that the GRB jet can break out a very massive Pop III star if it is a blue supergiant (BSG) progenitor, for which accretion from the long-lived hydrogen envelope to the black hole plays a key role (see also Woosley & Heger 2012). Some peculiar GRBs like GRB 130925A may be well explained by a progenitor of this type as recently argued by Piro et al. (2014). The relevant question is whether or not a very massive Pop III star can end its life as a BSG, rather than an RSG. The BSG model of 915 $M_\odot$ used by Suwa & Ioka (2011) and Nagakura et al. (2012) is taken from Ohkubo et al. (2009, the Y-1 model), who constructed this model with rapid mass accretion from a 1 $M_\odot$ protostar. By contrast, in the present study as well as in the previous ones by Baraffe et al. (2001), Marigo et al. (2003), and YDL12, all Pop III stars with $M \gtrsim 300\,M_\odot$ become RSGs at the final stage for both non-

Table 3
Final Radius of Very Massive Stars for Different Mixing Parameters

M_i	v_{crit}/v_K	f_{over}	α_{semi}	M_f	$T_{eff,\,f}$	R_f
($M_\odot$)				($M_\odot$)	(K)	($R_\odot$)
300	0.9	0.000	0.04	251.9	3821	4761.8
300	0.9	0.335	1.00	264.0	4271	4769.8
500	0.8	0.000	0.04	469.8	7293	2550.6
500	0.8	0.335	1.00	464.9	4157	7022.7

Note. Each column has the following meaning: M_i: initial mass, v_{crit}/v_K: the critical rotation for the given Γ at the equatorial surface in units of the Keplerian value with rigid rotation, f_{over}: overshooting parameter. That is, the convective layer is extended by f_{over} times local pressure scale heights beyond the convectively unstable region, α_{semi}: semi-convection parameter as defined by Langer et al. (1983), M_f: final mass, $T_{eff,\,f}$: final effective temperature, R_f: final radius.

rotating and rotating cases, unless they lose most of their hydrogen envelopes. This result seems robust given that each group used a different prescription for overshooting, semi-convection and rotation. To further investigate how the final radius varies with different assumptions on the overshooting and semi-convection, we calculated a couple of models without overshooting and a small semi-convection parameter ($\alpha_{semi} = 0.04$) with 300 $M_\odot$ and 500 $M_\odot$ and compared them with our fiducial models. As presented in Table 3, this hardly causes any difference in the final radius for 300 $M_\odot$. A significant reduction in the final radius with no overshooting is found with 500 $M_\odot$ but it still does not become a BSG. This strong tendency to become an RSG might be related to the fact that very massive stars are very close to the Eddington limit: according to the equation of state, more expansion of a gas is needed to consume a given amount of energy input as the role of radiation pressure becomes more important.

The discrepancy between Ohkubo et al. (2009, in particular the result with their Y sequences) and the others is probably related to the rapid mass accretion throughout the whole evolutionary stages that was assumed in Ohkubo et al. This assumption is, however, subject to many uncertainties. For example, it is observed that in their M-1 sequence, for which mass accretion was stopped for $M \geqslant 321\,M_\odot$, the radius rapidly increases to $\sim$1000 $R_\odot$ during the post-main-sequence phase, unlike the case of the Y sequences where rapid mass accretion continues until the end of the evolution. Note that the M-1 sequence in Ohkubo et al. was constructed to consider the radiation feedback from the mass accreting star that can greatly reduce the mass accretion rate as discussed by McKee & Tan (2008). The feedback effect must become more complicated with rotation. In particular, mass accretion should result in accretion of angular momentum and the mass-accreting Pop III proto-stars could easily reach critical rotation when the mass grows beyond a certain limit. Given that mass accretion would be effectively halted once the stellar surface reaches the critical rotation, the Ohkubo et al.'s assumption of continuous mass accretion that gave the BSG solution is not likely to be valid with rotation. This issue will be addressed in a separate paper (H. Lee and S.-C. Yoon 2015, in preparation).

Our conclusion is still subject to modifications with binary interactions. For example, in a close binary system, the mass-accreting star may not be easily rejuvenated but have a relatively small core mass compared to the total mass, if mass accretion occurs near the end of the main sequence or during the post-main-sequence phase. This can often make the star remain blue during the late evolutionary stages (Podsiadlowski & Joss 1989; Braun & Langer 1995). The evolution of massive binary Pop III stars is thus an interesting topic of future work.

6. CONCLUSIONS

We discussed the possibility of super-collapsars using the evolutionary models of very massive Pop III stars. We find that Pop III stars with $M_i > 3000\,M_\odot$ cannot be born with enough angular momentum for collapsars in the core. This is mainly because these very massive stars are very close to the Eddington limit for which case the critical rotation velocity at the equatorial surface is severely limited to a value significantly below the Keplerian velocity. The potential progenitors for super-collapsars that can lead to energetic GRBs should have an initial mass range of $300\,M_\odot \lesssim M_i \lesssim 3000\,M_\odot$.

We have to consider the evolution of these stars to get a more realistic mass range for super-collapsar progenitors. High angular momentum and strong magnetic fields of large scales at the pre-collapse stage are the two essential conditions needed for super-collapsars (Komissarov & Barkov 2010; Mészáros & Rees 2010). Given that magnetic torques can lead to efficient braking of the stellar core, these two conditions may not be easily satisfied simultaneously (cf. Yoon et al. 2012). Our evolutionary models indeed show that the angular momentum condition can be fulfilled only when we ignore magnetic torques. If we only consider hydrodynamic processes for the transport of angular momentum like Eddington–Sweet circulations, the angular momentum conditions for super-collapsars at the final evolutionary stage can be fulfilled for the initial mass range of $300\,M_\odot \lesssim M_i \lesssim 700\,M_\odot$.

However, these stars become red supergiants at the pre-collapse stage and therefore production of an energetic gamma-ray burst from super-collapsar events seems difficult. If the core can retain enough angular momentum to produce relativistic jets, it may lead to a jet-powered type IIP supernova. If the initial rotational velocity is relatively low for the considered mass range, only the outermost layers of the hydrogen envelope may have specific angular momentum above the critical limit for collapsar. The consequent jet formation would produce an ultra-long (about a month), relatively faint ($L \sim 10^{47}$ erg s^{-1}), gamma-ray transient that is marked by a short spike in the gamma-ray luminosity ($L \sim 10^{49} - 10^{51}$ erg s^{-1}) during the last few seconds in the restframe.

This work was supported by the Basic Science Research (2013R1A1A2061842) program through the National Research Foundation of Korea (NRF).

REFERENCES

Abel, T., Bryan, G. L., & Norman, M. L. 2002, Sci, 295, 93
Alexander, D. R., & Ferguson, J. W. 1994, ApJ, 437, 879
Arlt, R., & Rüdiger, G. 2011, MNRAS, 412, 107
Baraffe, I., Heger, A., & Woosley, S. E. 2001, ApJ, 550, 890
Braithwaite, J. 2006, A&A, 449, 451
Braun, H., & Langer, N. 1995, A&A, 297, 484
Bromm, V., Coppi, P. S., & Larson, R. B. 2002, ApJ, 564, 23
Bromm, V., Yoshida, N., Hernquist, L., & McKee, C. F. 2009, Natur, 459, 49
Brott, I., de Mink, S. E., Cantiello, M., et al. 2011, A&A, 530, 115
Burrows, D. N., Kennea, J. A., Ghisellini, G., et al. 2011, Natur, 476, 421
Cantiello, M., Mankovich, C., Bildsten, L., Christensen-Dalsgaard, J., & Paxton, B. 2014, ApJ, 788, 93
Chatzopoulos, E., & Wheeler, J. C. 2012, ApJ, 748, 42
Cucchiara, A., Levan, A. J., Fox, D. B., et al. 2011, ApJ, 736, 7

Denissenkov, P. A., Pinsonneault, M., Terndrup, D. M., & Newsham, G. 2010, ApJ, 716, 1269
Eggenberger, P., Maeder, A., & Meynet, G. 2005, A&A, 440, L9
Eggenberger, P., Montalbán, J., & Miglio, A. 2012, A&A, 544, L4
Endal, A. S., & Sofia, S. 1976, ApJ, 210, 184
Freese, K., Ilie, C., Spolyar, D., Valluri, M., & Bodenheimer, P. 2010, ApJ, 716, 1397
Fryer, C. L., Woosley, S. E., & Heger, A. 2001, ApJ, 550, 372
Glatzel, W., Fricke, K. J., & el Eid, M. F. 1985, A&A, 149, 413
Greiner, J., Kühler, T., Fynbo, J. P. U., et al. 2009, ApJ, 693, 1610
Haemmerlé, L., Eggenberger, P., Meynet, G., Maeder, A., & Charbonnel, C. 2013, A&A, 557, A112
Heger, A., Langer, N., & Woosley, S. E. 2000, ApJ, 528, 368
Heger, A., & Woosley, S. E. 2002, ApJ, 567, 532
Heger, A., Woosley, S. E., & Spruit, H. 2005, ApJ, 626, 350
Hirano, S., Hosokawa, T., Yoshida, N., et al. 2014, ApJ, 781, 60
Hosokawa, T., Omukai, K., Yoshida, N., & Yorke, H. W. 2011, Sci, 334, 1250
Hosokawa, T., Omukai, K., & Yorke, H. W. 2012, ApJ, 756, 93
Iglesias, C. A., & Rogers, F. J. 1996, ApJ, 464, 943
Kawai, N., Kosugi, G., Aoki, K., et al. 2006, Natur, 440, 184
Komissarov, S. S., & Barkov, M. V. 2010, MNRAS, 402, L25
Kozyreva, A. 2014, PhD Thesis, University of Bonn
Kozyreva, A., Yoon, S.-C., & Langer, N. 2014, A&A, 566, 146
Kudritzki, R. P., Pauldrach, A., Puls, J., & Abbott, D. C. 1989, A&A, 219, 205
Langer, N., Fricke, K. J., & Sugimoto, D. 1983, A&A, 126, 207
Levan, A. J., Tanvir, N. R., Cenko, S. B., et al. 2011, Sci, 333, 199
MacFadyan, A., & Woosley, S. E. 1999, ApJ, 524, 262
Madau, P., & Rees, M. J. 2001, ApJL, 551, L27
Maio, U., & Barkov, M. V. 2014, MNRAS, 439, 3520
Marigo, P., Chiosi, C., & Kudritzki, R.-P. 2003, A&A, 399, 617
McKee, C. F., & Tan, J. C. 2008, ApJ, 681, 771
Mészáros, P., & Rees, M. J. 2010, ApJ, 715, 967
Meynet, G., & Maeder, A. 1997, A&A, 321, 465
Nagakura, H., Suwa, Y., & Ioka, K. 2012, ApJ, 754, 85
Nieuwenhuijzen, H., & de Jager, C. 1990, A&A, 231, 134
Ohkubo, T., Nomoto, K., Umeda, H., Yoshida, N., & Tsuruta, S. 2009, ApJ, 706, 1184
Omukai, K., & Palla, F. 2003, ApJ, 589, 677
Piro, L., Troja, E., Gendre, B., et al. 2014, ApJ, 790, 15
Podsiadlowski, Ph., & Joss, P. C. 1989, Natur, 338, 401
Quataert, E., & Kasen, D. 2012, MNRAS, 419, L1
Salvaterra, R., Della Valle, M., Campana, S., et al. 2009, Natur, 461, 1258
Schneider, R., Ferrara, A., Natarajan, P., & Omukai, K. 2002, ApJ, 571, 30
Spolyar, D., Bodenheimer, P., Freese, K., & Gondolo, P. 2009, ApJ, 705, 1031
Spruit, H. C. 2002, A&A, 381, 923
Stacy, A., Bromm, V., & Leob, A. 2011, ApJ, 730, 1
Stacy, A., Greif, T. H., & Bromm, V. 2012, MNRAS, 422, 290
Stacy, A., Greif, T. H., Klessen, R. S., Bromm, V., & Loeb, A. 2013, MNRAS, 431, 1470
Suijs, M. P. L., Langer, N., Poelarends, A.-J., et al. 2008, A&A, 481, 87
Suwa, Y., & Ioka, K. 2011, ApJ, 726, 107
Talon, S., Kumar, P., & Zahn, J. P. 2002, ApJL, 574, L175
Tanvir, N. R., Fox, D. B., Levan, A. J., et al. 2009, Natur, 461, 1254
Umeda, H., & Nomoto, K. 2002, ApJ, 565, 385
Woosley, S. E. 1993, ApJ, 405, 273
Woosley, S. E., & Heger, A. 2012, ApJ, 752, 32
Yoon, S.-C., Dierks, A., & Langer, N. 2012, A&A, 542, A113 [YDL12]
Zahn, J.-P., Talon, S., & Matias, J. 1997, A&A, 322, 320
Zahn, J.-P., Brun, A. S., & Mathis, S. 2007, A&A, 474, 145